Performance Evaluation of an Integrated Optoelectronic Receiver

A. Vera-Marquina[*1], J. Martínez-Castillo[2], I. E. Zaldívar-Huerta[3], A. Díaz-Sánchez[3]

[1] Departamento de Investigación en Física
Universidad de Sonora
Hermosillo, Sonora, México
*avera@guaymas.uson.mx
[2] Centro de Investigación en Micro y Nanotecnología
Universidad Veracruzana
Boca del Río, Veracruz, México
[3] Departamento de Electrónica
Instituto Nacional de Astrofísica, Óptica y Electrónica
Tonantzintla, Puebla, México

ABSTRACT

This work describes the optical and electrical characterization of an integrated optoelectronic receiver. The receiver is composed of a photodiode and a transimpedance amplifier, both fabricated in silicon technology using a 0.8 µm BiCMOS process. The total area occupied by the photodiode is of 10,000 µm^2. In a first step, the generated photocurrent of the photodiode is measured for the wavelengths of 780 nm and 830 nm at different levels of optical power. In a second step, the responsivity and quantum efficiency parameters of the photodiode are computed. Finally, an electrical measurement including the transimpedance amplifier is achieved. A potential application for this optoelectronic receiver is on the first optical communications window.

Keywords: Optoelectronic receiver, photodiode, optoelectronic integrated circuit, BiCMOS.

RESUMEN

Este artículo describe la caracterización óptica y eléctrica de un receptor optoelectrónico integrado. El receptor comprende un fotodiodo y un amplificador de transimpedancia, ambos fabricados en silicio utilizando tecnología de proceso BiCMOS de 0.8 µm. El área total utilizada por el fotodiodo es de 10,000 µm^2. Inicialmente, se mide la fotocorriente generada por el fotodiodo para las longitudes de onda de 780 nm y 830 nm a diferentes niveles de potencia óptica. Posteriormente, se calculan los parámetros de responsividad y eficiencia cuántica del fotodiodo. Finalmente, se realiza una medición eléctrica que involucra al amplificador de transimpedancia. Una aplicación potencial para este receptor optoelectrónico se encuentra en la primera ventana de comunicaciones ópticas.

1. Introduction

Currently, data transmission standards have an important role in optical communication systems. For this reason, an efficient design of the input stage is a critical issue for optoelectronic systems. An integrated input stage is composed of a superficial photodiode (PD) and a transimpedance amplifier (TIA) in a single chip, which is known as an optoelectronic integrated circuit (OEIC) [1]. The main characteristics required for an input stage are: high gain, extended bandwidth, low power consumption, minimum noise contributions and reduced area requirements. In this sense, optical and electrical devices fabricated in silicon technology allow satisfying the requirements previously cited [2-3]. The maturity of silicon technology represents a powerful platform that is truly compatible with standard CMOS processing [4-5], and by consequence, very attractive from the economic point of view. In this sense, the goal of this work resides in achieving a full performance evaluation of an integrated optoelectronic receiver that was designed by one of the authors [6]. This optoelectronic receiver is composed of a PD and a TIA fabricated in silicon technology in a 0.8 µm BiCMOS process. The main advantage to use this technology resides in the fact that low-power supplies are used in relation to bipolar technology, solving in this way problems related to power consummation. In a first step, optical measurements are carried out, and then electrical measurements involving the amplifier are achieved.

Normally, photodetectors and transimpedance amplifiers are built in a separate way. In this work, we are presenting an electro-optical device that comprises both. An optical and electrical characterization was achieved guaranteeing in this way a complete performance. It is very important to remark that the measurements achieved are at a prototype level. The fabricated photodiode operates well at the wavelength of 830 nm that corresponds to the first window optical communication, for this reason this electro-optical device has a potential application as a receptor module in an optical link. If well is truth that this wavelength is reserved only for short optical links, currently Local Area Network (LAN) operates at this wavelength allowing in this way a fast process of information.

2. Receiver operating principle

Figure 1 illustrates the basic scheme of an optical stage reception. The PD converts the incident optical power to an electrical current which is amplified by the TIA, obtaining in this way a corresponding voltage level (V_o) at its output. The feedback resistance (R_f) connected between the output and input of the TIA is used for amplification purposes.
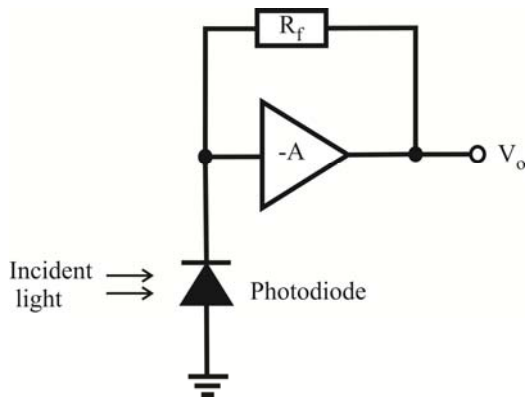

Figure 1. Basic scheme of an optical stage reception

2.1 Photodiode operation

The PD was fabricated in a standard technology using a bulk process, and the diffused *pn* junctions are close to surface, as shown in Figure 2. An n-well region has been used to isolate the detector from substrate. The PD operates in avalanche mode to obtain an amplified signal and noise reduction. Since the p^{++} is used as collect layer,

the *pn* junction is close to the surface and the photodiode area can be easily illuminated by using a multimode or monomode optical fiber.
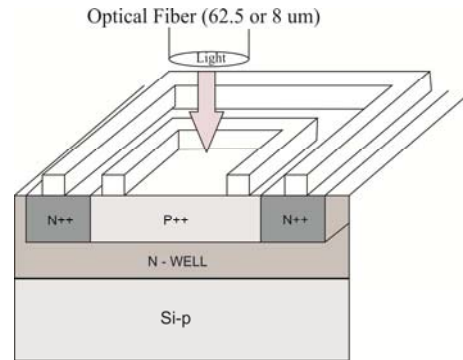

Figure 2. Photodiode cross-section

The equivalent circuit corresponding to a PD is illustrated in Figure 3, where I_p is the generated photocurrent, I_d is the dark current, C_s is the junction capacitance, R_s, R_{sh}, and R_L, are the series, sheet and load resistance, respectively.
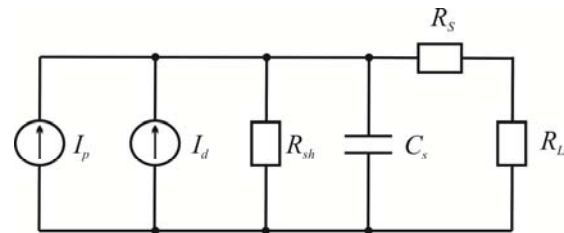

Figure 3. Equivalent photodiode circuit

Since $X_{C_s} \ll R_{sh}$ at high frequencies and assuming that R_s is less than 100Ω because it represents the contact resistance, which was reduced by layout techniques and the resistance of the undepleted silicon, model of Figure 3 can be simplified to the equivalent circuit shown in figure 4. R_L was substituted for the input impedance of the TIA.
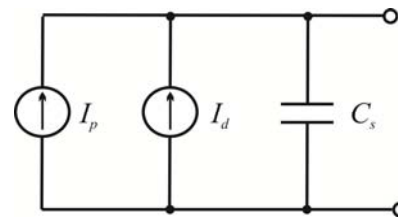

Figure 4. Simplified photodiode small signal model

The responsivity parameter of the PD can be computed as [7]

$$\Re = \frac{I_p}{P_0} = \frac{\eta q}{h\nu} \qquad (1)$$

where P_o is the incident optical power, η is the quantum efficiency, q is the electron charge, $h\nu$ is photon energy, and the quantum efficiency can be evaluated by

$$\eta = \frac{1.24\Re}{\lambda} \qquad (2)$$

3. Transimpedance amplifier operation

The CMOS TIA structure used in this work is based on the common-gate topology, using negative feedback. Because a negative feedback is used at the input transistor, the bandwidth is increased and the noise contributions are reduced. The TIA amplifier diagram is shown in Figure 5.
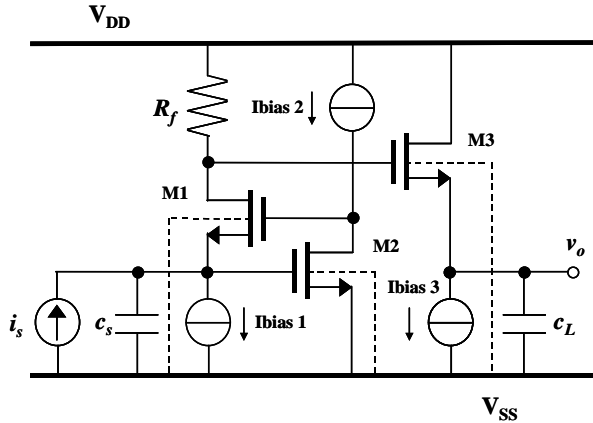

Figure 5. Modified common-gate structure TIA applications in OEIC systems

The transfer function achieved by using a local feedback network is in Equation (3)

$$\frac{v_{out}}{i_s} =$$

$$\frac{g_{m2}g_{m1}}{\left(sc_{p1} + g_{f1}\right) * \left\{ s^2 \left[c_{gd2} + c_{gs1} \right] \left[c_s + c_{gs2} \right] + s \left[c_{gd2} + c_{gs1} \right] g_{m2} + g_{m2}g_{m1} \right\}} \qquad (3)$$

where i_s is the photogenerated current including I_p and I_d, g_{m1} and g_{m2} are transconductances of

transistors M1 and M2, respectively. The c_{gd2} and c_{gs2} are the gate-drain and gain-source capacitances of the transistor M2, respectively. The c_{gs1} is the gain-source capacitance of the transistor M1. The c_{p1} and c_s are the output load and photodiode capacitances, respectively, and finally the g_{f1} is the load resistance of the TIA amplifier. The TIA gain is given by R_f when $s \rightarrow 0$. A transimpedance gain of 40 dB and a bandwidth of 2 GHz were obtained using an R_f of 100Ω and a output capacitance of 0.3 pF. A further description of the design of the TIA is given in [6].

4. Description of the optoelectronic integrated circuit

This integrated optoelectronic receiver monolithically integrates a PD and a preamplifier circuit. Process BiCMOS AMS technology is used for this purpose using minimum dimensions of 0.8 μm. Figure 6 shows a photograph of the integrated optical stage receptor in which the PD and the TIA are indicated.
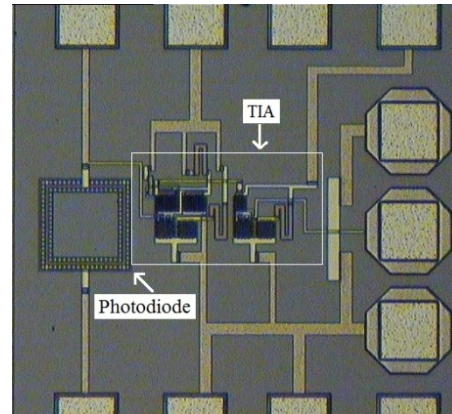

Figure 6. Photograph of the integrated optical stage receptor

As was previously mentioned, this manufacturing process allows the *pn* junction to be very near the surface allowing the PD area to be illuminated independently of the TIA. Figure 7 corresponds to a zoom of the last photograph corresponding only to the PD. Its dimensions are 100 μm x100 μm.

The chip containing the optoelectronic integrated circuit is glued on a FR4 substrate, and the pads are welded to the lines of a printed circuit in order to allow its connection to the electrical equipment. Figure 8 corresponds to a picture of this prototype.
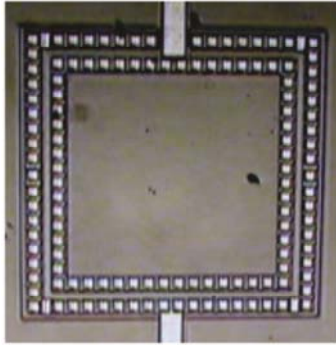
Figure 7. Photograph showing only
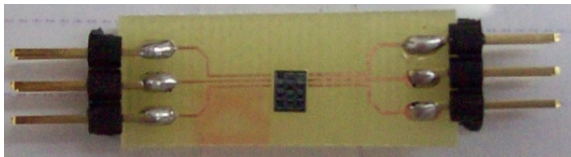the photodiode area

Figure 8. Picture of the chip glued
on the FR4 substrate

Figure 9 shows a zoom of the optoelectronic integrated circuit where detail of the interconnection between pads and connection lines is clearly observable.
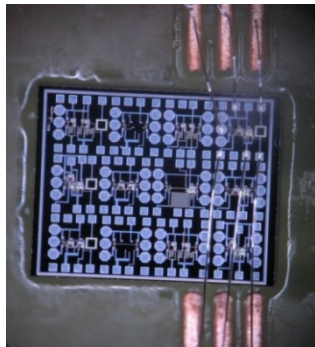

Figure 9. Zoom of the chip showing the interconnection between pads and connection lines

4.1 Measuring of the photocurrent

Electrical and optical characterization is an important step because provides information that allows corroborates the good performance of the

device. In this sense, in the following a complete optical and electrical characterization is described. For this goal we have used an Electro/Optical Converter (Gravizon model LL-780GI, λ=780 nm), and a modulable laser unit (Lasiris, λ=830 nm). A visible sensor head (Thorlabs, model S120A) is attached to an optical power meter system (Thorlabs, model S110), in order to verify the wavelength and measure the optical power of the devices previously mentioned. Optical powers of P=640 µW and P=40 mW are measured for the Electro/Optical Converter and the modulable laser unit, respectively. Figure 10 corresponds to the experimental setup used to measure the photocurrent of the photodiode. The light issued from the laser is coupled to a segment of standard multimode optical fiber (62.5 µm/0.27) and attached to a test point in order to guide the light as near as possible to the PD area. An external amperimeter (Keithley multimeter, model 2001) closes the circuit under measure in order to record the values of current. A variable DC source (+V) allows a DC sweep in the range of 0 to -18V.
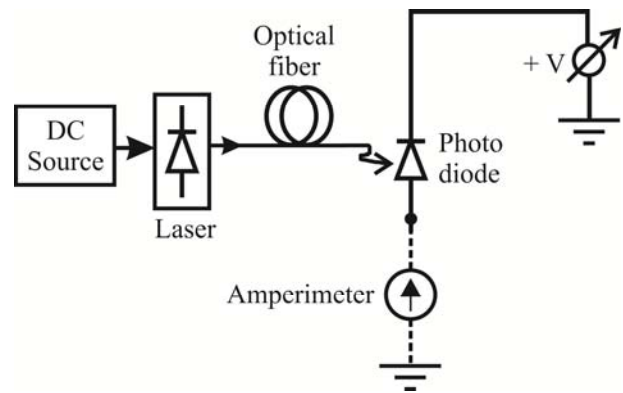

Figure 10. Experimental setup to measure the photocurrent generated

In a first step, the PD is polarized in reverse-bias in order to measure the reverse leakage photocurrent (or dark current) produced without illumination. Figure 11 corresponds to the measured current level whose range is in nanoampers, and the breakdown voltage is located around -17 V.
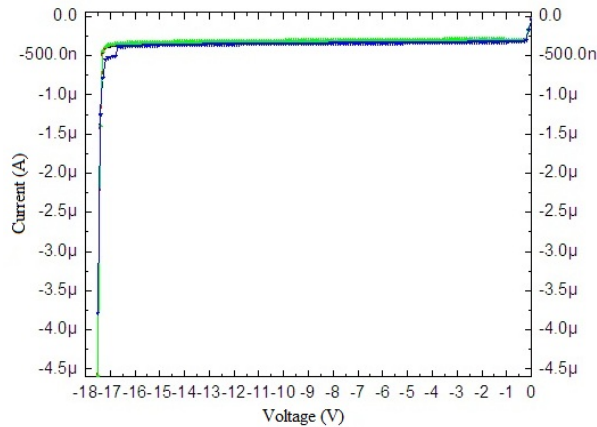
Figure 11. Measured dark current of the photodiode

In a second step, the PD is illuminated by using the electro/optical converter Gravizon. Its corresponding results are illustrated in Figure 12. In this case, the photocurrent value is increased because of the illumination and is in the order of microampers.
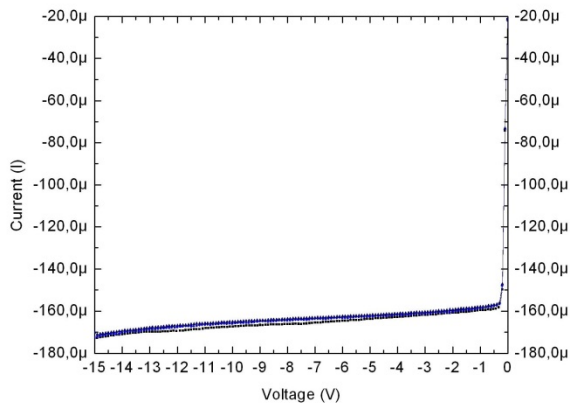

Figure 12. Measured generated photocurrent corresponding to λ=780 nm, and P=640 μW

Finally, the PD is now illuminated by using the modulable laser unit. Figure 13 plots the measured photocurrent. In this case and because of the high incident optical power, the values of current in the order of milliamps is remarkable.
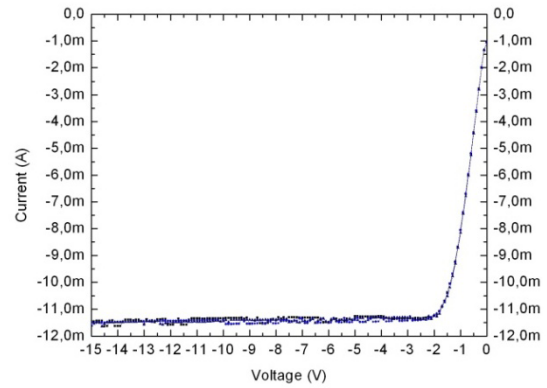

Figure 13. Measured generated photocurrent corresponding to λ= 830 nm, and P=40 mW

4.2 Evaluation of the quantum efficiency

Once the levels of photocurrent are known, for simplicity, the photons reflected at the face of the photodiode are omitted. The responsivity and quantum efficiency are determined from Equation (1) and (2), respectively. Table 1 shows these results.

Case	λ (nm)	P_0	I_p	$\Re$ (A/W)	η
1	780	640 μW	170 μA	0.26	0.422
2	830	40 mW	11.5mA	0.28	0.430

Table 1. Summary of experimental results corresponding to the photocurrent, responsivity and quantum efficiency parameters

The low value corresponding to the responsivity parameter is justified by the absence of an antireflectance film at the face of the photodiode.

5. Transimpedance amplifier stage

As was previously mentioned, the integrated optoelectronic receiver monolithically integrates a PD and a preamplifier circuit, which is shown in Figure 14, which illustrates the experimental setup used to test the optoelectronic stage including the amplifier. In this case, the amplifier is operated as follower voltage. The electro/optical converter is modulated by a sinusoidal signal by using a signal generator (Rhode & Schwarz, Model SM101).
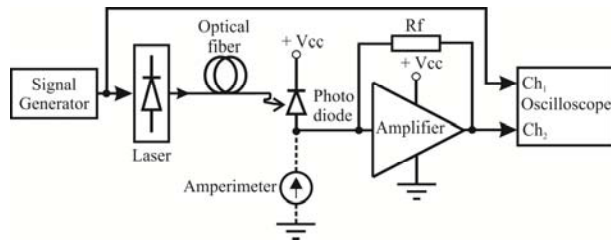
Figure 14. Experimental setup used to measure the response of the amplifier stage

The input of the amplifier is short-circuited to its output in order to operate as follower voltage. The modulated light issue of the E/O converter is coupled again to a segment of standard multimode optical fiber in order to illuminate the area of the photodiode. The polarization voltage (V_{cc}) applied to the photodiode is fixed to -3 volts. Channel 1 of an oscilloscope (Tektronix, TDS3054B) allows monitoring the sinusoidal signal (f=1.589 MHz and V_{pp}=1.14 V) applied to the E/O converter, whereas channel 2 permits recovering the output signal. Upper and lower traces illustrated in Figure 15 correspond to the screen of the oscilloscope showing the applied and recovered signal, respectively. A good result without a noticeable degradation is clearly observable.
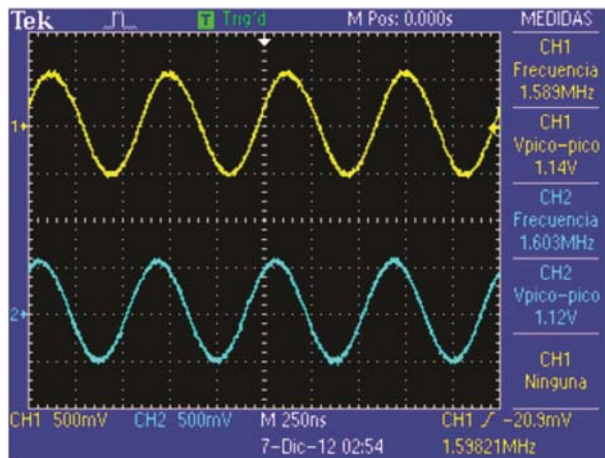

Figure 15. Resulting waveforms when the amplifier is configured as follower voltage

Figure 16 shows a comparison between the simulated and experimental result of the frequency response of the optical system. In the experimental test, measurements were made using a Wiltron vector-analyzer model 360 and a Tektronix S-

parameters test model 576. A bandwidth of 1.9GHz and 0.8GHz was obtained by simulated and experimental ways, respectively.
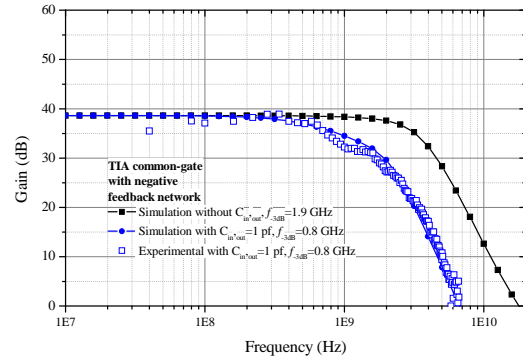

Figure 16. Simulated and experimental frequency response of the TIA

6. Conclusions

A full optical and electrical characterization of an integrated optoelectronic receiver was achieved. It is well known that a factor that affects the number of photon incidents, and thus the quantum efficiency, is the absence of an anti-reflection coating on the surface of the photodiode; hence, the values computed for this device are within an acceptable range. It is true that the quantum efficiency could be increased by increasing the thickness of the intrinsic region to allow more absorption of photons, but the price would be to increase the response time of the device. On the other hand, the moderate frequency response of the device is justified by the technique used to illuminate the photodiode and the interconnection lines to the FR4 substrate. However, this can be improved if the optical fiber is launched directly over the photodiode area. It is clear that the optical wavelengths used for this characterization correspond to the first optical window communications; therefore, this integrated optoelectronic receiver is found to have a potential and practical application in this window.

References

[1] R. Soref, Applications of silicon-based optoelectronics, MRS Bull., 1998, pp. 20–24.

[2] S. Radovanovic, A.-J. Annema, B. Nauta, 3Gb/s monolithically integrated photodiode and pre-amplifier in standard 0.18 μm CMOS, Proceedings of the IEEE Solid-State Circuit Conference, 2004, Vol. 1, pp. 472-540.

[3] F. Aznar, S. Celma, B. Calvo, A 0.18 μm CMOS 1.25 Gbps front-end receiver for low-cost short reach optical communications, Proceedings of the IEEE 36th European Solid-State Circuits Conference, Vol. 1, 2010, pp. 554-557.

[4] T. Heide, A. Ghazi, H. Zimmermann, and P. Seegebrech, Monolithic CMOS Photoreceivers for Short-Range Optical Data Communications, Electronics Letters, Vol. 35, 2000, pp. 1655-1656.

[5] S. Radovanovic, A-J. Annema, B. Nauta, Bandwith of integrated photodiodes in standard CMOS for CD/DVD applications, Microelectronics Reliability, Vol. 45, 2005, pp. 705-710.

[6] J. Martínez-Castillo, P. García-Ramírez, and A. Díaz-Sánchez, "Two MOS Opto-Electronic Structures for High-Frequency Applications", XX Conference on Design of Circuits and Integrated Systems, DCIS 2005, Lisboa, Portugal.

[7] Gerd Keiser, Optical Fiber Communications, McGraw-Hill, 2010, pp. 244-249.